

Peptide-Induced Lipid Flip-Flop in Asymmetric Liposomes Measured by Small Angle Neutron Scattering

Michael H. L. Nguyen,[†] Mitchell DiPasquale,[†] Brett W. Rickeard,[†] Milka Doktorova,[‡] Frederick A. Heberle,^{‡,§,||} Haden L. Scott,^{§,||} Francisco N. Barrera,^{||} Graham Taylor,^{||} Charles P. Collier,^{||,#} Christopher B. Stanley,^{||,V} John Katsaras,^{O,◆,¶} and Drew Marquardt^{*,†,+,ID}

[†]Department of Chemistry and Biochemistry, University of Windsor, Windsor, N9B 3P4 ON Canada

[‡]Department of Integrative Biology and Pharmacology, University of Texas Health Science Center at Houston, Houston, Texas 77225, United States

[§]Center for Environmental Biotechnology, University of Tennessee, Knoxville, Tennessee 37996, United States

^{||}Department of Biochemistry & Cellular and Molecular Biology, University of Tennessee, Knoxville, Tennessee 37996, United States

⁺The Bredesen Center, University of Tennessee, Knoxville, Tennessee 37996, United States

[#]Center for Nanophase Materials Sciences, Oak Ridge National Laboratory, Oak Ridge, Tennessee 37831, United States

^VNeutron Scattering Division, Oak Ridge National Laboratory, Oak Ridge, Tennessee 37831, United States

^OLarge Scale Structures Group, Oak Ridge National Laboratory, Oak Ridge, Tennessee 37831, United States

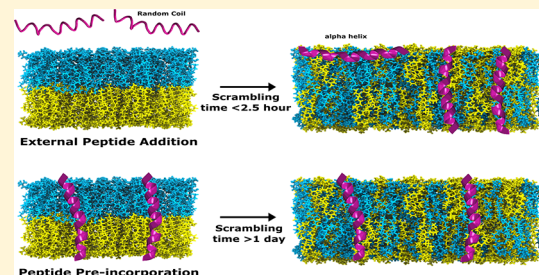
[◆]Shull Wollan Center, a Joint Institute for Neutron Sciences, Oak Ridge National Laboratory, Oak Ridge, Tennessee 37831, United States

[¶]Department of Physics and Astronomy, University of Tennessee, Knoxville, Tennessee 37996, United States

^{*}Department of Physics, University of Windsor, Windsor, N9B 3P4 ON Canada

S Supporting Information

ABSTRACT: Despite the prevalence of lipid transbilayer asymmetry in natural plasma membranes, most biomimetic model membranes studied are symmetric. Recent advances have helped to overcome the difficulties in preparing asymmetric liposomes *in vitro*, allowing for the examination of a larger set of relevant biophysical questions. Here, we investigate the stability of asymmetric bilayers by measuring lipid flip-flop with time-resolved small-angle neutron scattering (SANS). Asymmetric large unilamellar vesicles with inner bilayer leaflets containing predominantly 1-palmitoyl-2-oleoyl-*sn*-glycero-3-phosphocholine (POPC) and outer leaflets composed mainly of 1,2-dimyristoyl-*sn*-glycero-3-phosphocholine (DMPC) displayed slow spontaneous flip-flop at 37 °C (half-time, $t_{1/2} = 140$ h). However, inclusion of peptides, namely, gramicidin, alamethicin, melittin, or pHLIP (i.e., pH-low insertion peptide), accelerated lipid flip-flop. For three of these peptides (i.e., pHLIP, alamethicin, and melittin), each of which was added externally to preformed asymmetric vesicles, we observed a completely scrambled bilayer in less than 2 h. Gramicidin, on the other hand, was preincorporated during the formation of the asymmetric liposomes and showed a time resolvable 8-fold increase in the rate of lipid asymmetry loss. These results point to a membrane surface-related (e.g., adsorption/insertion) event as the primary driver of lipid scrambling in the asymmetric model membranes of this study. We discuss the implications of membrane peptide binding, conformation, and insertion on lipid asymmetry.



INTRODUCTION

In Nature the two lipid bilayer leaflets of cell plasma membranes possess chemically distinct lipids, thus making the overall membranes asymmetric (an example of a model asymmetric bilayer is depicted in Figure 1a). Glycerophospholipids, a major component of lipid bilayers, can differ from one another as follows: (i) degree of acyl chain unsaturation and length; (ii) headgroup chemistry; and (iii) type of bond (ester or ether) connecting the acyl chains to their glycerol

backbone. With differing glycerophospholipid compositions, physical and chemical differences arise between the bilayer leaflets, which affect membrane fluidity and structure and have been shown to influence membrane function and membrane-associated protein activity.^{1,2}

Received: May 30, 2019

Revised: July 28, 2019

Published: August 13, 2019



Maintaining membrane asymmetry is energetically expensive for cells and is accomplished by ATP-fueled proteins such as flippases and floppases.³ Loss of asymmetry can lead to cell death or apoptosis. Specifically, the migration of phosphatidylserine (PS) lipids from the inner to the outer bilayer leaflet is a trigger for phagocytosis of dying cells.^{4,5} Interestingly, greater protein reconstitution rates and activities are seen when studying asymmetric liposomes when compared to their symmetric counterparts.^{6,7} Thus, in recent years, there has been an increasing number of studies examining the role of lipid asymmetry on different proteins and peptides.^{8–10} On the other hand, studies examining how macromolecules affect membrane asymmetry are much less common.¹⁰

Beyond the relevant enzymes present in cells, we address the role that antimicrobial peptides (AMPs) have on lipid flip-flop. AMPs are a highly conserved group of amphipathic peptides and an integral part of the immune system of most, if not all, species of life. Their mode of action is primarily based on disrupting key plasma membrane properties and functions, such as electrochemical gradients, cell motility, and shape through lysis.¹¹ In order to do so, many will first bind and then insert themselves into the membrane, sometimes forming higher ordered structures (e.g., pores) to permeabilize the membrane. However, under certain conditions they have also been shown to accelerate lipid flip-flop,^{10,12–16} which is thought to be pertinent to their cytotoxic effects.¹⁷ To our knowledge, no existing study decouples the role of peptide binding to membranes and their transmembrane inserted state on lipid flip-flop dynamics. This study will shed light on the mechanism through which AMPs disrupt membranes, highlighting the possibility of lipid reorganization as a relevant cause of cell death.

Considerable research has been performed on passive, active, and non-enzyme-catalyzed lipid flip-flop in order to gain an understanding of the energy needed to generate, maintain, and disrupt lipid asymmetry. Many of these studies used spin- or fluorescent-labeled lipids because of their widespread availability.^{3,12,18–20} However, bulky fluorescent probes can potentially perturb the membrane and alter its physical properties, affecting lipid flip-flop in the process.^{21,22} Furthermore, these techniques measure the translocation of the reporter lipid, which is physically and chemically different from the host lipid of interest.²² As a result, probe-free techniques such as sum-frequency vibrational spectroscopy (SFVS)^{22,23} and neutron reflectometry²⁴ have gained some prominence as they allow measurements of lipid kinetics without the use of extrinsic probes. Collectively, these techniques are sensitive to chemical differences in leaflets by using isotopically labeled lipids that better resemble those found in nature.

Recently, we developed a novel probe-free assay using proton NMR to measure the relative flip-flop rates of phosphatidylcholine (PC) lipids in stress- and defect-free unilamellar vesicle systems.²⁵ The passive flip-flop rates were measured in large unilamellar vesicles (LUVs) with an asymmetric distribution of isotopically labeled phospholipids. Using this system, flip-flop rates were found to be orders of magnitude slower than those measured on substrate-supported planar bilayers. The difference between the two sample preparations was attributed to incomplete substrate coverage in the case of planar bilayers that led to the formation of pore defects.²⁵ Unlike passive lipid flip-flop, pores allow lipids to move from one leaflet to the other by simple diffusion without

desolvating their headgroups. The NMR approach, however, is currently limited to choline-containing lipid systems. Moreover, in the case of proteolipidic systems, charged amino acid residues can potentially chelate with the NMR shift reagent (Pr^{3+}), adversely affecting not only the NMR signal but also protein conformation, binding, insertion, and function. Currently, we are not aware of a probe-free technique that measures lipid flip-flop rates in asymmetric vesicles in a non-headgroup specific fashion.

To address this, we explored the use of SANS, a technique that is differentially sensitive to hydrogen's isotopes, namely protium and deuterium (^1H and ^2H , respectively), to measure lipid flip-flop in PC bilayers. Isotopic substitution of ^1H for ^2H imparts neutron contrast to the system that can then be used to study structural and dynamical membrane features. For example, SANS has been used to study the existence of lipid domains in living bacterial membrane²⁶ and the thickness of membranes reconstituted from natural lipid sources,^{26,27} including symmetric²⁸ and asymmetric model membranes.^{29–31} Although the use of SANS to measure lipid flip-flop rates is not a novel concept,³² until now it has only been applied to symmetric model membranes.^{32–36} This is partly due to the technical difficulties associated with preparing asymmetric vesicles of sufficient amounts and concentrations,^{37,38} and the complicated experimental setup and subsequent analysis of scattering profiles.

Here we describe a novel SANS approach to measure lipid flip-flop in asymmetric LUVs (aLUVs). As a proof of concept, we first characterized aLUVs composed of PC lipids to ensure that the neutron scattering signal was sufficiently different from that of symmetric (scrambled) control samples. We then introduced peptides with different modes of membrane interactions. For example, gramicidin (gA) forms ion channels when dimerized, and at elevated concentrations alamethicin (Alm) and melittin (Mel) form barrel-stave and toroidal pores, respectively.³⁹ Although pHLIP is not an AMP, it was chosen to represent both an unstructured peripheral peptide and a transmembrane helix, depending on pH. For example, at neutral pH, pHLIP adsorbs to the membrane surface but inserts into the membrane at low pH.⁴⁰ Initially, peptide influence on lipid asymmetry was tracked through the time-dependent loss of the scattering signal, indicative of increased lipid flip-flop that, ultimately, results in a scrambled bilayer. Importantly, the lipid scrambling effect was most pronounced when the peptides were externally added to aLUVs, compared to when they were incorporated during aLUV preparation. Our results lend insights to the study of proteolipidic systems, especially with regard to peptide binding, conformation, and insertion on lipid bilayer asymmetry.

MATERIALS AND METHODS

Materials. 1,2-Dimyristoyl-d54-*sn*-glycero-3-phosphocholine [14:0(d27)/14:0(d27) PC, dC-DMPC] and 1-palmitoyl-2-oleoyl-*sn*-glycero-3-phosphocholine-d13 (16:0/18:1 PC-d13, dH-POPC) were purchased from Avanti Polar Lipids, Inc. (Alabaster, AL) and used as received. Methyl- β -cyclodextrin (M β CD) was purchased from Acros Organics (Thermo Fisher Scientific, Waltham, MA). The centrifugal filter device, Amicon Ultra-15, was purchased from EMD Millipore (Billerica, MA). Deuterated methanol (D-methanol) and 99.9% D₂O were purchased from Cambridge Isotopes (Andover, MA). Praseodymium(III) nitrate hexahydrate (Pr³⁺) was purchased from Alfa Aesar (Ward Hill, MA) and prepared as a 20 mM stock solution in D₂O. Alamethicin and melittin were purchased from Sigma-Aldrich (St. Louis, MO) and kept as stock solutions in D-methanol.

Gramicidin was purchased as a lyophilized powder from Sigma-Aldrich (Oakville, ON, Canada) and kept as a stock solution in methanol. pHILIP was purchased as a lyophilized powder from P3 Biosystems (Louisville, KY) with 95% purity as verified by reverse-phase high performance liquid chromatography (HPLC). Sodium deuterioxide (NaOD) and deuterium chloride (DCl) were purchased from Sigma-Aldrich (St. Louis, MO).

Preparation of Asymmetric LUV Samples. aLUVs were prepared using a slightly modified methyl- β -cyclodextrin mediated exchange protocol from that outlined by Doktorova and co-workers.^{29,37} Briefly, dC-DMPC and dH-POPC (with 5 mol % POPG) in HPLC-grade chloroform were dried into separate lipid films under a stream of nitrogen gas and left overnight in vacuo to remove any traces of solvent. The dC-DMPC and dH-POPC films were then hydrated using 20% (w/w) sucrose and 20 mM NaCl solutions, respectively. dH-POPC acceptor LUVs (which “accept” outer leaflet lipids from donor vesicles) were extruded (31 passes) using 100 nm pore diameter disposable polycarbonate membranes (NanoSizer extruder, T&T Scientific). In the presence of M β CD (at a M β CD/donor nominal ratio of 8/1), dC-DMPC donor multilamellar vesicles (MLVs) were incubated for 1 h with acceptor dH-POPC LUVs (at a 3/1 donor-to-acceptor molar ratio) to promote outer leaflet exchange. During this process, aLUVs with dH-POPC primarily in the inner leaflet and dC-DMPC in the outer leaflet gradually form from the acceptor LUVs. Following this, aLUVs were purified through a combination of centrifugation and centrifugal filtration where the H₂O buffer solution was exchanged for D₂O to reduce neutron background signal. The final concentration of aLUVs was determined to be 17 mg/mL based on total intensity measured by dynamic light scattering (DLS) versus samples of known concentrations.

gA from a methanol stock solution was added at a peptide-to-lipid (P/L) molar ratio of 1/40 during the lipid film preparation step (i.e., preincorporated into the acceptor vesicles as described in Doktorova et al.¹⁰). It should be noted that the addition of gA in methanol to preformed aLUVs resulted in instantaneous peptide aggregation and was thus not used. In contrast, Alm and Mel precipitated out of solution during the centrifugation steps of the asymmetric vesicle preparation, and could not be incorporated directly into asymmetric bilayers, as was done in the case of gA. Alm and Mel were therefore introduced to preformed aLUVs using D-methanol at a P/L ratio of 1/40. The D-methanol concentration in the sample was ~3% (v/v), which, by itself, did not induce scrambling in aLUVs (see Figure S4). As previously described, monomeric pHILIP transitions from a mostly unstructured peptide adsorbed to the membrane to an α -helical conformation when it inserts into the membrane at low pH.^{41,42} In order to take advantage of these pH-sensitive conformers, aLUVs in a 10 mM sodium phosphate buffer solution (pH 7.9) were added to a lyophilized pHILIP powder (weighed mass) at a P/L ratio of 1/150 and incubated for up to 1 h. Afterward, the pH of the different aLUVs preparations was adjusted to alter pHILIP’s resulting orientation from one that is membrane adsorbed (pH 7.9) to a transmembrane orientation (pH 4.6). Measurements at pH 6.0 were also performed to capture any intermediate state(s) of pHILIP.⁴⁰ pHILIP’s secondary structures in these different pH conditions was determined using circular dichroism (Figure S3).

Quantifying aLUV Composition by GC/MS and Solution ¹H NMR. To determine the lipid exchange efficiency of the asymmetric sample preparation, aLUV lipid compositions were analyzed using a combination of gas chromatography/mass spectrometry (GC/MS) and ¹H NMR. A small aliquot of ~20 μ g of lipids was subjected to transesterification using acid-catalyzed methanolysis.²⁹ The relative populations of the free fatty acid chains were determined using GC/MS²⁹ to yield the overall fraction of dC-DMPC and dH-POPC. GC/MS measurements were performed on an Agilent 5890A gas chromatograph (Santa Clara, CA) outfitted with a 5975C mass spectrometer. Taking advantage of the unique retention times of chemically distinct acyl chains, aLUVs were determined to possess 38% dC-DMPC and 62% dH-POPC. The exchange efficiency of the

asymmetric prep was thus 76%, in good agreement with previous reports.^{25,29,43}

¹H NMR was used to determine the interleaflet lipid distribution of dC-DMPC and, combined with the GC/MS results, the overall lipid composition of each leaflet. NMR measurements were carried out at 50 °C with an Avance III 600 MHz spectrometer (Bruker, Billerica, MA). Spectra were acquired using the Bruker TopSpin software and analyzed using TopSpin 3.5. The outer and inner leaflet distribution of protonated PC headgroups was determined through the addition of a 2 μ L aliquot of 20 mM Pr³⁺ into 700 μ L of aLUVs with a concentration of ~1 mg/mL. The addition of Pr³⁺ causes outer leaflet choline peaks to shift downfield. NMR spectra were fit with a sum of Lorentzians; the peaks representing the inner and outer leaflet cholines were then integrated to determine their areas, which are directly proportional to the mole fraction of dC-DMPC in the outer and inner bilayer leaflets (0.87 and 0.13, respectively). NMR spectra are shown in Figure S1. The fact that some donor dC-DMPC is present in the inner leaflet is not unexpected and is in line with previous observations.³⁷ A summary of the NMR data can be found in Table S1 in the Supporting Information.

aLUV Structure Determined by DLS and Small Angle Scattering. DLS measurements to determine vesicle integrity in the presence of peptides and solvent as a function of time were conducted on a Brookhaven BI-200SM system (Brookhaven Instruments, Holtsville, NY). For the DLS measurements, aLUVs at a concentration of 17 mg/mL were diluted by a factor of 1000 using ultrapure water and measured at room temperature. Small angle X-ray scattering (SAXS) experiments on aLUV and aLUV-peptide samples at 17 mg/mL were performed using a Rigaku BioSAXS-2000 (Rigaku Americas, The Woodlands, TX) equipped with a Pilatus 100 K detector and an HF007 rotating copper anode. Several measurements of each sample were conducted at 37 °C and examined for radiation damage before averaging. SAXS and SANS data (of the first time points) were jointly refined using an asymmetric six-slab model that accounts for contributions from the lipid headgroups, acyl chains, and terminal methyls of each leaflet to derive the structural parameters shown in Figure S2.³⁰ aLUV control samples were well-fit by the asymmetric model, while those containing peptides were best-fit by a symmetric bilayer.

Time-Resolved Flip-Flop Using SANS. SANS measurements were conducted on the extended Q-range small angle neutron scattering (EQ-SANS) diffractometer located at the Spallation Neutron Source, Oak Ridge National Laboratory (ORNL, Oak Ridge, TN). The sample-to-detector distance was set to 1.6 m and the incident neutron wavelength, λ , at 4–8 Å, resulting in a q -range of 0.02–0.8 Å⁻¹, where q is the scattering vector and is determined as follows:

$$q = \frac{4\pi \sin \theta}{\lambda} \quad (1)$$

where 2θ is the angle of scattered neutrons with respect to the incident beam. Here, 1 mm path length quartz banjo cells (Hellma USA, Plainview, NY) were used, and neutrons were measured, collected, and counted on a 2D ³He detector. Scattering data were circularly averaged to produce a 1D scattering intensity curve as a function of q . The data were corrected for empty cell and D₂O background, sample transmission, and detector pixel sensitivity using the ORNL Mantid software.⁴⁴

aLUVs with and without peptides were studied using SANS to determine lipid flip-flop rates. Flip-flop rates in the presence of pHILIP at different pH conditions were also studied. Lipid samples of 17 mg/mL concentration were measured at 37 °C for 1 h to collect sufficient counting statistics high- q .

Modeling and Quantifying Lipid Flip-Flop Rates. During SANS measurements, neutron scattered intensity $I(q)$ was monitored as a function of q . At low- q , $I(q)$ is dominated by the size and shape of the LUVs, while at high- q the signal is primarily due to the average structure normal to the plane of the bilayer (e.g., bilayer thickness). In our case, the scattered intensity at high- q is enhanced by the interleaflet contrast due to bilayer asymmetry, as shown in Figure 1.

A normalized intensity decay scheme was used to quantify changes in scattered intensity as a function of time, as given by the normalized total intensity, $\Delta I(t)/\Delta I(0)$,³²

$$\frac{\Delta I(t)}{\Delta I(0)} = \frac{\sqrt{I(t)} - \sqrt{I(\infty)}}{\sqrt{I(0)} - \sqrt{I(\infty)}} \quad (2)$$

where $I(t)$ is the integrated area underneath the scattering curve at time t after the start of experimentation. $I(0)$ and $I(\infty)$ represent, respectively, the integrated area at $t = 0$ of an aLUV sample and after bilayer asymmetry is lost. The $I(\infty)$ time point is of the same lipid composition as our time-resolved samples, but the lipids are homogeneously mixed instead of asymmetrically distributed. Because we are interested in observing changes to the bilayer as a result of lipid flip-flop, the total scattering intensity at each time point was determined by integrating the area under the scattered signal in the q -range $0.1\text{--}0.4 \text{ \AA}^{-1}$, where the difference in scattering intensity of asymmetric and symmetric LUVs is most pronounced. Plotting the normalized intensities as a function of time results in a decay curve that can be fitted using one parameter to determine the lipid flip-flop rate constant, k_f i.e.,

$$\frac{\Delta I(t)}{\Delta I(0)} = e^{(-2k_f t)} \quad (3)$$

The flip-flop half time is then calculated as

$$t_{1/2} = \frac{\ln 2}{2k_f} \quad (4)$$

Determining Secondary Peptide Structure Using Circular Dichroism. Circular dichroism (CD) was used to determine the secondary structure of the different peptides after SANS and SAXS experimentation (see Figure S3). CD spectra were acquired using a Jasco (Easton, MD) J-815 spectropolarimeter equipped with a Peltier system. Spectra were acquired at 37°C using a 2 mm cuvette at a scan rate of 100 nm/min, recording 20–40 acquisitions. The final lipid concentration was 1 mM. Raw data were converted into a mean residue ellipticity using

$$[\theta] = \frac{\theta}{10l(N-1)} \quad (5)$$

where θ is the measured ellipticity, l is the path length of the cell in cm, c is the protein concentration in M, and N is the number of amino acids. Appropriate lipid blanks were subtracted in all cases.

RESULTS

Lipid Flip-Flop Can Be Monitored with SANS Using Asymmetric Vesicles with Interleaflet Hydrogen/Deuterium Contrast. To monitor lipid flip-flop using time-resolved SANS, we first sought to determine if major scattering differences exist between aLUVs and symmetric LUVs. It is well-known that the aLUV scattering form factor has minima with nonzero intensity, in contrast to that of symmetric LUVs.⁴⁵ Previous studies have used this feature to identify lipid asymmetry and build models to fit such data, extracting key bilayer parameters and leaflet compositions.^{29,30,46}

Figure 1b shows modeled $I(q)$ curves based on LUVs with equal fractions of dH-POPC (deuterated headgroup) and dC-DMPC (perdeuterated acyl chains) at 37°C . The model accounts for the scattering contributions from the individual bilayer leaflets.³⁰ Figure 1b shows a substantial intensity increase in the q -range $0.15\text{--}0.3 \text{ \AA}^{-1}$ for bilayers containing an asymmetric distribution of dH-POPC in the inner leaflet and dC-DMPC in the outer leaflet. To demonstrate this experimentally, we produced different model systems in order to mimic and maximize the dynamic range observed between the modeled asymmetric and symmetric curves. These

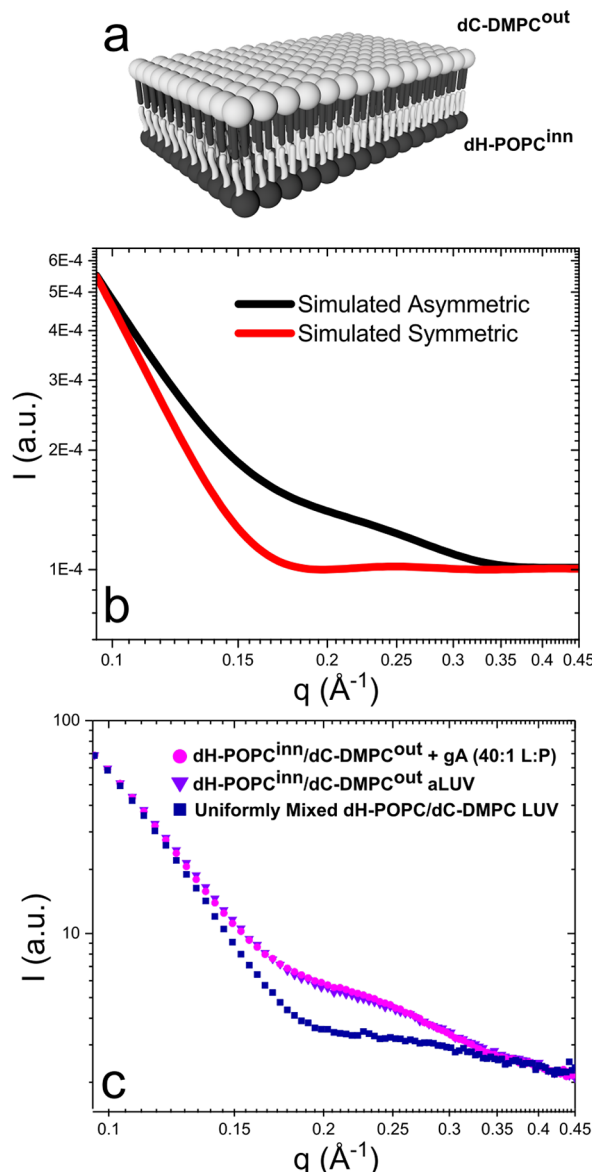


Figure 1. (a) Cartoon of an asymmetric bilayer. Dark shaded components indicates deuterated moieties. (b) Predicted neutron scattering curves of asymmetric ($\text{dH-POPC}^{\text{inn}}/\text{dC-DMPC}^{\text{out}}$) and symmetric vesicles calculated using a six-slab bilayer model.³⁰ (c) $I(q)$ scattering data from three different samples: (1) compositionally asymmetric LUVs with their inner leaflets composed mainly of dH-POPC and outer leaflet of dC-DMPC (pink circles); (2) aLUVs with a 1/40 P/L ratio of gA (purple triangles); and (3) uniformly mixed LUVs with same dH-POPC and dC-DMPC ratios (navy squares). Scattering curves are overlaid to highlight similarities and differences.

systems possessed either isotopic asymmetry, i.e., the same lipid species but different isotopic labeling (not shown), or compositional asymmetry, where the individual leaflets possess chemically different lipid species.

Of the different samples studied, the aLUVs composed of dH-POPCⁱⁿⁿ/dC-DMPC^{out} (Figure 1a) possessed the greatest dynamic scattering range, as can be seen from the high- q data ($0.1\text{--}0.4 \text{ \AA}^{-1}$) shown in Figure 1c. Compared to its relatively featureless scrambled counterpart, these aLUVs display appreciable “uplift” in scattering intensity in the vicinity of the first minima ($\sim 0.18 \text{ \AA}^{-1}$), which we attribute to the asymmetric distribution of lipids with different chemical

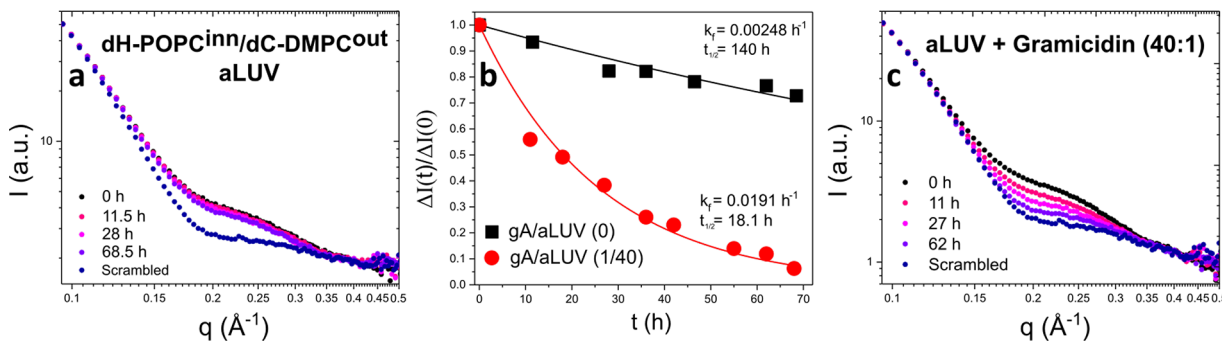


Figure 2. High- q SANS data as a function of time showing an aLUV control (peptide-free, a). All measurements were conducted at $37\text{ }^{\circ}\text{C}$ for 1 h. For clarity purposes, not all measured curves are shown. (b) Normalized total intensity decay as a function of time in hours. Two plots are shown: aLUVs in the absence (black squares) and presence of gA (red circles) (P/L ratio of 1/40). Decays are the result of passive and peptide-enhanced lipid flip-flop, respectively. Continuous bold lines are best fits to the data used to determine the flip-flop rate constant (k_f) and flip-flop half-time ($t_{1/2}$). (c) Gramicidin-incorporated aLUVs at a P/L of 1/40.

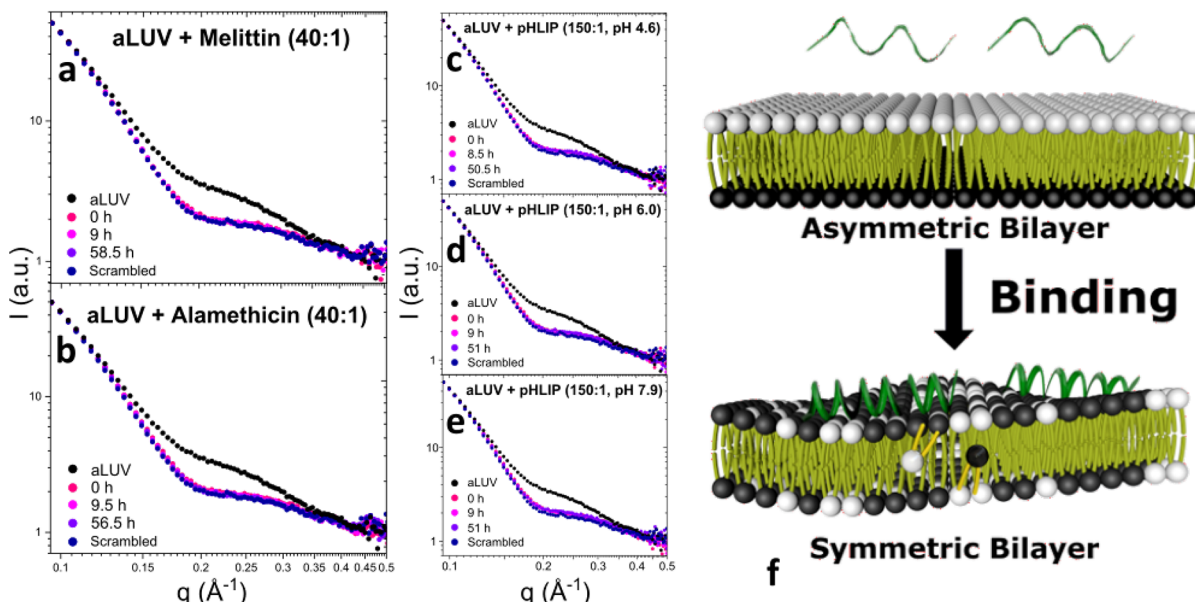


Figure 3. (a–e) High- q SANS data as a function of time showing aLUV scattering curves after the external addition of melittin (a), alamethicin (b), and pHILIP (c–e). The individual L/P ratios are displayed in each graph. All measurements were conducted at $37\text{ }^{\circ}\text{C}$. For clarity purposes, not all measured curves are shown. (f) Cartoon of proposed mechanism of peptide-induced lipid flip-flop. Shown in the top panel of (f) are the peptide monomers in a random coil conformation and an asymmetric bilayer composed of chemically distinct leaflets. Peptide binding, shown in the bottom, initiates a conformational change from a random coil to α -helical. This adsorption, and likely subsequent insertion events, leads to bilayer reorganization and loss of lipid asymmetry.

makeups (Figure 1b). This dynamic range was deemed suitable to monitor the bilayer transition from asymmetric to symmetric. Importantly, the modeled data bears a strong resemblance to the experimental data (Figure 1b) and any minor differences can be attributed to potential deviations in lipid composition, bilayer thickness, polydispersity, and background scattering between the model and experimental.

A Transmembrane Peptide Preincorporated into Asymmetric Vesicles Increases the Rate of Lipid Flip-Flop. Control aLUVs and aLUVs with gA preincorporated were prepared separately, yet both scatter similarly as a function of q (Figure 1c). This finding, coupled with the minimal loss of gA seen in this type of asymmetric proteoliposome preparation,¹⁰ lends confidence for this method of sample preparation for studies using SANS. It was also observed that gA in its transmembrane state does not contribute noticeably to the neutron scattering intensity,

meaning the measured ensemble average of the bilayer structure is unchanged. Although it is known that gA causes bilayer thinning or thickening depending on the conditions,⁴⁷ these deformations are likely to occur locally and, as a result, could not be detected by SANS in the present study or SAXS previously.¹⁰

Over the course of almost 3 days, the leaflet compositions of unperturbed fluid-phase aLUVs are practically unaltered as the aLUV scattering intensity data only show a slight decay (Figure 2a). Because a complete minima decay was not collected, due to experimental time constraints often associated with SANS experimentation, an $I(\infty)$ time point (representing a homogeneously mixed LUV of the same overall lipid composition, as shown in Figure 2) was used to normalize the integrated area of the intensity curves. Fits using eq 3 on the normalized integrated intensity from Figure 2a revealed a flip-flop rate constant of $2.48 \times 10^{-3} \text{ h}^{-1}$, as shown in Figure

2b. Converting the flip-flop rate constant to half-time using eq 4, the calculated half-time of 140 h for peptide-free aLUVs is in good agreement with previous NMR results,¹⁰ albeit slower than those found with LUVs doped with fluorescent or spin labeled lipids^{18,19,48} and orders of magnitude slower than the rates reported for supported bilayers.^{22–24} When compared to the flip-flop half-times found by Nakano et al. in free-floating vesicles (DMPC $t_{1/2} = \sim 8.5$ h, POPC $t_{1/2} > 1000$ h both at 37 °C),^{32,33} our aLUVs display a $t_{1/2}$ much slower than pure DMPC, but slightly faster than flip-flop in POPC vesicles.

As shown in Figure 2c, preincorporation of gA into aLUVs resulted in an accelerated decay of the scattered intensity, indicative of a continuous loss of membrane asymmetry. Fitting the normalized integrated total intensity showed that the presence of transmembrane gA reduced the flip-flop half-time from 140 to 18.1 h, an almost 8-fold reduction in $t_{1/2}$ and in good agreement with differential scanning calorimetry and NMR data.¹⁰

Externally Added Peptides Result in Rapid and Complete Loss of Lipid Asymmetry. We also carried out experiments where aLUV controls were mixed either with Mel, Alm, or pHLIP (at three different pH values) to determine the effects of membrane-surface events (such as binding and insertion) on bilayer asymmetry. Interestingly, the scattering curves did not decay in the same manner as observed with gA. In fact, the aLUV–peptide curves in Figure 3a–e resemble those of the scrambled LUV control; i.e., the aLUVs lost their asymmetry within the first hour after preparation. The key differences between them are the method of peptide addition and peptide species: gA was incorporated during aLUV formation, Mel and Alm (Figure 3a and b, respectively) introduced to aLUVs using D-methanol, and pHLIP powder to aLUVs in phosphate buffer with the addition of DCl to adjust the pH (Figure 3c–e). Regardless, the samples, where the peptide was added externally after the aLUVs were prepared, display the same effects on aLUV scattering. Specifically, bilayer asymmetry was affected over the same time period, regardless of differences in the peptide's physical state or concentration, solvent type, pH, or mode of action.

As we altered pHLIP's orientation from surface-bound to partially inserted and then to inserted (as indicated by CD; see Figure S3), we observe the same bilayer scrambling effects of the PC lipids, which is depicted in Figure 3c–e. It therefore appears that bilayer scrambling results from an event that is not associated with pHLIP's secondary structure or membrane partitioning. In pHLIP's case, lipid flip-flop appears to be headgroup dependent as previous results have suggested that pHLIP does not promote flip-flop of PS lipids.⁹ We rationalize this by the fact that PS and pHLIP are both negatively charged and thus repel each other.⁴⁹ Since only PS distribution was monitored in the previous study, the effect of pHLIP on PC flip-flop was not elucidated.

We also looked into any potential loss of asymmetry as a result of having methanol in solution. Using time-resolved SANS and symmetric protiated and deuterated DMPC vesicles, we previously showed that methanol at volumes as low as 0.5% increases the rate of DMPC vesicle mixing, and, in turn, DMPC flip-flop.⁵⁰ In those experiments, liposomal mixtures were incubated with methanol for 1 h prior to mixing of the two isotopic DMPC populations. Aiming to learn whether enhanced lipid dynamics also occur in aLUVs, the maximum administered volume (3% v/v) of methanol, used to introduce Alm and Mel, was added to peptide-free aLUVs.

Here, the introduction of methanol was followed by SANS measurement to capture any immediate lipid scrambling. The resulting SANS scattering pattern revealed no substantial decay in the first SANS minima (see Figure S4), which indicates that methanol is not the primary driver of bilayer scrambling, pointing instead to a predominantly peptide-mediated mechanism of lipid flip-flop observed in this study. The present result is not necessarily a contradiction to our past work. One hour (the time aLUV samples were measured on SANS here) of data collection only produces 10–20% of the total intensity decay curve in pure symmetric DMPC vesicles.⁵⁰ In other words, in both symmetric and asymmetric instances, D-methanol did not initiate an immediate and complete scrambling of lipid bilayers. To note, samples containing gA and pHLIP were methanol-free.

To further verify that peptides were the primary cause of lipid scrambling, we monitored for the possibility of vesicle fusion, which can potentially increase the rate of lipid bilayer scrambling. Besides pHLIP,⁴¹ the other peptides studied are known to promote vesicle fusion,⁵¹ especially at concentrations of $P/L \geq 1/50$.⁵² However, DLS measurements taken prior to peptide addition and after incubation dismiss this possibility, as the average particle diameter was unaffected (data not shown). This result also rules out the “carpet” mechanism where vesicles disintegrate into polydisperse peptidolipid structures.⁵³ We can thus confidently conclude that the observed changes in scattering are due to lipid flip-flop and not the result of large-scale structural reorganization.

■ DISCUSSION

As mentioned, the externally added peptides interact with the membrane through very different mechanisms. However, regardless of their mode of action, amino acid sequence, length, and conformation, they all disrupt membrane asymmetry, hinting at a general mode of action. Even though pHLIP is not an AMP, it is possible that pHLIP and AMPs share certain features that allow them to disrupt membrane asymmetry despite differences in how they interact with membranes. Our findings point to this scenario—one which implies that perhaps all natural and *de novo* peptides and proteins may be capable of causing substantial lipid flip-flop.

It has been suggested that any membrane-interacting molecules, at sufficient quantities, are able to influence membrane properties⁵⁴ by compromising the mechanical integrity of the bilayer. Therefore, at high peptide-to-lipid ($P/L \geq 1/40$) concentrations, changes to the membrane may be due to an overwhelming number of peptides interacting simultaneously with the membrane and not necessarily a specific AMP mode of action. However, with respect to the current study, the nonpore forming pHLIP at a P/L ratio of 1/150 refutes this possibility. At this nonmembrane permeabilizing concentration,⁵⁵ the peptide was seen to eliminate membrane asymmetry, while the presence of gA in the membrane at higher concentrations ($P/L = 1/40$) did not rapidly scramble the bilayers. Instead, we observed a gradual loss of asymmetry. Our data therefore suggest that the enhanced lipid flip-flop observed for pHLIP, Alm, and Mel is related to their activity at the membrane surface (see Figure 3f).

For lytic AMPs, an initial mode of action involves interaction with cellular membranes. Most AMPs begin in the aqueous extracellular matrix as randomly coiled monomers and undergo a conformational change upon contact with the membrane,

forming a variety of secondary structures that allow for peptide penetration and eventual membrane permeation. However, few studies have looked into the potential of peptide binding to the membrane as a disrupter of lipid asymmetry. Fattal et al. suggested that if a “perturbation mode” of action (also known as *interfacial activity*, where peptides in a nonoligomeric, surface-bound state disturb the physicochemical properties of adjacent lipids⁵⁴) indeed existed, lipid flip-flop would occur upon peptide binding to the bilayer¹² – a notion in agreement with the data presented in the current study. Decoupling the binding and transmembrane steps showed that the peptides that underwent a binding step initiated rapid and complete lipid asymmetry loss, in contrast to the gA case.

At similar P/L concentrations, gA did not cause 7-nitrobenz-2-oxa-1,3-diazol-4-yl (NBD) conjugated PC lipids to experience “appreciable” lipid flip-flop¹² (>96 h), suggesting gA is better capable of enhancing the translocation of biologically relevant lipids than those modified covalently. This difference can be attributed either to an unfavorable steric interaction between the NBD fluorophore and the peptide, or that the bulkiness of the fluorophore impede movement through the peptide-induced defect. In Figure 2b, gA (18.1 h) and gA-free (140 h) half-times show an almost 8-fold decrease when gA is preincorporated into aLUVs. This result is, for the most part, in good agreement with that of Anglin and co-workers (2–10 fold increase in gel-phase di18:0 PC bilayers). The similarity in time scales (hours) yet difference in lipid phase-state (fluid vs gel) is intriguing as the rate of lipid flip-flop has been shown to be phase-dependent,^{18,25} with flip-flop in gel-phase membranes being much slower. Bilayer geometry, incomplete surface coverage in planar bilayers, and possible substrate–lipid interactions in supported bilayers are possible explanations for these difference in time-scales.^{14,25,36} Nevertheless, gA activity appears to be independent of lipid phase state.

In its surface-adsorbed state, pHLIP can perturb lipid membranes to a greater extent than when inserted.⁵⁵ This may also be true for Alm and Mel, which can adopt a surface-bound state.⁵⁶ In their monomeric forms, Alm and Mel are embedded just below the lipid headgroups, lying parallel to the membrane plane (not inserted).⁵⁷ In this surface-bound state, they induce membrane thinning⁵⁷ that can compromise membrane integrity by creating local defects that can accelerate lipid flip-flop, a notion that is in agreement with previous reported findings.^{25,58}

A surface-adsorbed peptide that lies below the headgroups would change the effective area of that (outer) leaflet, which would lead to global stresses across the membrane. This area imbalance may then result in disruption of the sustained partitioning of the hydrophobic and hydrophilic regions present in the bilayer, allowing for the transbilayer movement of solutes, peptides, and lipids.⁵⁴ This type of stress (normal to the bilayer plane) is different from that produced by gA, possibly leading to the different outcomes observed here. As previously described,¹⁰ gA-induced stress (directed radially outward from the transmembrane peptide) comes from the high gA concentration (P/L = 1/40) at which, because of the local deformations around gA, the bilayer is unable to relax to its unperturbed state, since the gA dimers are too close to one another. These local deformations enhance the formation of defects, which reduces the free energy barrier to lipid flip-flop by destabilizing adjacent bilayer structure and/or lipid packing near the peptide.¹⁰ We postulate that the interfacial activity of a peptide on the membrane surface induces a far greater stress

upon the bilayer than when in its transmembrane state. This postulation is corroborated by a finding in which the number of lipids affected by adsorbed pHLIP is a factor of ~5–10 greater than that of transmembrane pHLIP.⁵⁹ We thus believe there exists a direct correlation between the amount of stress induced by the peptide (which seems dependent on its orientation) and its ability to propagate lipid flip-flop events.

At a critical P/L concentration, AMPs will transition from laying on the membrane surface to inserting themselves into the membrane, spanning both bilayer leaflets.⁵⁶ In the present study, Alm and Mel are seen to primarily adopt an α -helical structure and thus inserted orientation (see Figure S3). This is significant, as what was suggested previously,¹⁶ the act of peptide insertion can help transfer lipids across bilayer leaflets as lipids can be cotransported with the plunging peptide. Along with the potential for dynamic conversion between inserted and noninserted states, the cotransport process should be very effective at disrupting lipid organization.

This insertion step, as well as membrane binding, is missing in the case of gA as it was already preincorporated into the bilayer. We speculate that adding gA externally would yield similar results on the basis that the other three peptides examined differ drastically in amino acid composition and sequence length. Furthermore, as seen with pHLIP, a specific secondary structure and pore-formation are not prerequisites to causing complete lipid scrambling; thus, the delayed formation of helical gA channels (due to the accumulation of gA on the outer leaflet, instead of being present on both leaflets) would not affect the bilayer scrambling process as gA inserts itself into the bilayer.

An interesting point to note, with regards to the flip-flop halftime measured here for POPC and DMPC aLUVs, the observed value of ~140 h is magnitudes slower than in pure DMPC LUVs³² and faster than the imperceptible POPC flip-flop.³³ Taking into consideration interleaflet coupling,⁸ we suggest that the POPC-enriched leaflet may suppress lipids in the DMPC-enriched leaflet from flipping inward, giving rise to the observed half-time. Lipid flip-flop is known to be affected by bilayer thickness, among other properties.^{8,18} In this case, either the thicker POPC inner leaflet is inhibiting DMPC from flipping inward or, because POPC is not undergoing lipid flip-flop, there is an equal exchange of DMPC between the leaflets to compensate for any leaflet area imbalance, resulting in a lack of net change in leaflet composition. The equal exchange of DMPC between leaflets is possible because some outer leaflet lipids will leak into the inner leaflet during aLUV formation (~5–10%), allowing for the bidirectional diffusion of DMPC. Ultimately, the introduction of lipid asymmetry is seen to influence both POPC and DMPC translocation rates.

Though the current study does not provide unequivocal support for a peptide-based mechanism of lipid flip-flop, it does provide insights regarding membrane-peptide interactions affecting bilayer asymmetry and their possible importance in biological membranes. AMP action does not always lead to complete membrane destruction, which has clearly been demonstrated by the present SANS and DLS data. In search of another plausible mechanism, we delved into the action of AMPs onto lipids, specifically their dynamics and overall organization within the bilayer. Complete lipid scrambling of asymmetrically organized lipid bilayers was found. For lipid scrambling to be of biological relevance in the action of AMPs, a fast, or even immediate, effect is needed and desirable—one which precedes the permeabilization of the membrane. This

study shows that such a case is possible. Our findings also reveal the importance of evaluating vesicle asymmetry in studies involving peptides and proteins as peptide reconstitution was shown to destabilize the organizational integrity of aLUVs.

CONCLUSIONS

Although there are a number of different techniques that can measure lipid flip-flop, there are few that can do so in a probe-free and nonheadgroup specific manner. Here, we demonstrated how SANS could be used to reliably monitor lipid flip-flop in aLUVs made of dH-POPCⁱⁿⁿ/dC-DMPC^{out}. In these vesicles, lipid flip-flop half-times approaching 6 days were observed, in good agreement with some previous results and in contrast with those obtained from supported bilayers. The preincorporation of gA into aLUVs increased lipid flip-flop rates by a factor of almost 8, compared to peptide-free aLUVs. The addition of Alm, Mel, and pHLIP (at three different pH conditions) also eliminated membrane asymmetry. Importantly, it was shown that peptides adsorbed to membrane surfaces may have a much greater effect on lipid flip-flop than when inserted. This result highlighted a possible general mechanism of AMP action, which may be important to initiating cell death.

ASSOCIATED CONTENT

Supporting Information

The Supporting Information is available free of charge on the ACS Publications website at DOI: [10.1021/acs.langmuir.9b01625](https://doi.org/10.1021/acs.langmuir.9b01625).

Detailed experimental results and theory (PDF)

AUTHOR INFORMATION

Corresponding Author

*E-mail: drew.marquardt@uwindsor.ca.

ORCID

Frederick A. Heberle: [0000-0002-0424-3240](https://orcid.org/0000-0002-0424-3240)

Charles P. Collier: [0000-0002-8198-793X](https://orcid.org/0000-0002-8198-793X)

Christopher B. Stanley: [0000-0002-4226-7710](https://orcid.org/0000-0002-4226-7710)

Drew Marquardt: [0000-0001-6848-2497](https://orcid.org/0000-0001-6848-2497)

Notes

The authors declare no competing financial interest.

ACKNOWLEDGMENTS

Part of this research was conducted at ORNL's Spallation Neutron Source, sponsored by the Scientific User Facilities Division, Office of Basic Energy Sciences, U.S. Department of Energy. SAXS, DLS, and NMR measurements were supported by DOE scientific user facilities. This work was funded, in part, by the University of Windsor startup funds to D.M. M.D. and M.H.L.N. are both supported by Ontario Graduate Scholarships (OGS). D.M. acknowledges the support of the Natural Sciences and Engineering Research Council of Canada (NSERC) [funding reference number RGPIN-2018-04841]. This work was partially supported by NIH Grant R01GM120642 (F.N.B.) and NSF Grant MCB-1817929 (F.A.H.). J.K. is supported through the Scientific User Facilities Division of the Department of Energy (DOE) Office of Science, sponsored by the Basic Energy Science (BES) Program, DOE Office of Science, under Contract No. DEAC05-00OR22725. This manuscript has been authored

by UT-Battelle, LLC under Contract No. DE-AC05-00OR22725 with the U.S. Department of Energy. The United States Government retains and the publisher, by accepting the article for publication, acknowledges that the United States Government retains a nonexclusive, paid-up, irrevocable, worldwide license to publish or reproduce the published form of this manuscript, or allow others to do so, for United States Government purposes. The Department of Energy will provide public access to these results of federally sponsored research in accordance with the DOE Public Access Plan (<http://energy.gov/downloads/doe-public-access-plan>).

REFERENCES

- (1) Manno, S.; Takakuwa, Y.; Mohandas, N. Identification of a functional role for lipid asymmetry in biological membranes: Phosphatidylserine-skeletal protein interactions modulate membrane stability. *Proc. Natl. Acad. Sci. U. S. A.* **2002**, *99*, 1943–1948.
- (2) Lhermusier, T.; Chap, H.; Payrastre, B. Platelet membrane phospholipid asymmetry: from the characterization of a scramblase activity to the identification of an essential protein mutated in Scott syndrome. *J. Thromb. Haemostasis* **2011**, *9*, 1883–1891.
- (3) Seigneuret, M.; Devaux, P. F. ATP-dependent asymmetric distribution of spin-labeled phospholipids in the erythrocyte membrane: relation to shape changes. *Proc. Natl. Acad. Sci. U. S. A.* **1984**, *81*, 3751–5.
- (4) Martin, S. J. Early redistribution of plasma membrane phosphatidylserine is a general feature of apoptosis regardless of the initiating stimulus: inhibition by overexpression of Bcl-2 and Abl. *J. Exp. Med.* **1995**, *182*, 1545–1556.
- (5) Zwaal, R. F. A. Membrane and lipid involvement in blood coagulation. *Biochim. Biophys. Acta, Rev. Biomembr.* **1978**, *515*, 163–205.
- (6) Kamiya, K.; Kawano, R.; Osaki, T.; Akiyoshi, K.; Takeuchi, S. Cell-sized asymmetric lipid vesicles facilitate the investigation of asymmetric membranes. *Nat. Chem.* **2016**, *8*, 881.
- (7) Yanagisawa, M.; Iwamoto, M.; Kato, A.; Yoshikawa, K.; Oiki, S. Oriented reconstitution of a membrane protein in a giant unilamellar vesicle: experimental verification with the potassium channel KcsA. *J. Am. Chem. Soc.* **2011**, *133*, 11774–11779.
- (8) Marquardt, D.; Geier, B.; Pabst, G. Asymmetric lipid membranes: towards more realistic model systems. *Membranes* **2015**, *5*, 180–196.
- (9) Scott, H. L.; Heberle, F. A.; Katsaras, J.; Barrera, F. N. Phosphatidylserine Asymmetry Promotes the Membrane Insertion of a Transmembrane Helix. *Biophys. J.* **2019**, *116*, 1495–1506.
- (10) Doktorova, M.; Heberle, F. A.; Marquardt, D.; Rusinova, R.; Sanford, R. L.; Peyear, T. A.; Katsaras, J.; Feigenson, G. W.; Weinstein, H.; Andersen, O. S. Gramicidin Increases Lipid Flip-Flop in Symmetric and Asymmetric Lipid Vesicles. *Biophys. J.* **2019**, *116*, 860–873.
- (11) Béven, L.; Wroblewski, H. Effect of natural amphipathic peptides on viability, membrane potential, cell shape and motility of molluscs. *Res. Microbiol.* **1997**, *148*, 163–175.
- (12) Fattal, E.; Parente, R. A.; Szoka, F. C.; Nir, S. Pore-Forming Peptides Induce Rapid Phospholipid Flip-Flop in Membranes. *Biochemistry* **1994**, *33*, 6721–6731.
- (13) Taylor, G.; Nguyen, M. A.; Koner, S.; Freeman, E.; Collier, C. P.; Sarles, S. A. Electrophysiological interrogation of asymmetric droplet interface bilayers reveals surface-bound alamethicin induces lipid flip-flop. *Biochim. Biophys. Acta, Biomembr.* **2019**, *1861*, 335–343.
- (14) Anglin, T. C.; Liu, J.; Conboy, J. C. Facile lipid flip-flop in a phospholipid bilayer induced by gramicidin A measured by sum-frequency vibrational spectroscopy. *Biophys. J.* **2007**, *92*, L01–3.
- (15) Sapay, N.; Bennett, W. F.; Tieleman, D. P. Molecular simulations of lipid flip-flop in the presence of model transmembrane helices. *Biochemistry* **2010**, *49*, 7665–7673.

- (16) Matsuzaki, K.; Yoneyama, S.; Murase, O.; Miyajima, K. Transbilayer transport of ions and lipids coupled with mastoparan X translocation. *Biochemistry* **1996**, *35*, 8450–8456.
- (17) Hwang, B.; Hwang, J. S.; Lee, J.; Kim, J. K.; Kim, S. R.; Kim, Y.; Lee, D. G. Induction of yeast apoptosis by an antimicrobial peptide, Papiliocin. *Biochem. Biophys. Res. Commun.* **2011**, *408*, 89–93.
- (18) John, K.; Schreiber, S.; Kubelt, J.; Herrmann, A.; Müller, P. Transbilayer Movement of Phospholipids at the Main Phase Transition of Lipid Membranes: Implications for Rapid Flip-Flop in Biological Membranes. *Biophys. J.* **2002**, *83*, 3315–3323.
- (19) Kornberg, R. D.; McConnell, H. M. Inside-outside transitions of phospholipids in vesicle membranes. *Biochemistry* **1971**, *10*, 1111–1120.
- (20) Kol, M. A.; van Laak, A. N. C.; Rijkers, D. T. S.; Killian, J. A.; de Kroon, A. I. P. M.; de Kruijff, B. Phospholipid Flip Induced by Transmembrane Peptides in Model Membranes Is Modulated by Lipid Composition. *Biochemistry* **2003**, *42*, 231–237.
- (21) Devaux, P. F.; Fellmann, P.; Hervé, P. Investigation on lipid asymmetry using lipid probes: Comparison between spin-labeled lipids and fluorescent lipids. *Chem. Phys. Lipids* **2002**, *116*, 115–134.
- (22) Liu, J.; Conboy, J. C. 1,2-diacyl-phosphatidylcholine flip-flop measured directly by sum-frequency vibrational spectroscopy. *Biophys. J.* **2005**, *89*, 2522–2532.
- (23) Anglin, T. C.; Cooper, M. P.; Li, H.; Chandler, K.; Conboy, J. C. Free energy and entropy of activation for phospholipid flip-flop in planar supported lipid bilayers. *J. Phys. Chem. B* **2010**, *114*, 1903–1914.
- (24) Gerelli, Y.; Porcar, L.; Lombardi, L.; Fragneto, G. Lipid Exchange and Flip-Flop in Solid Supported Bilayers. *Langmuir* **2013**, *29*, 12762–12769.
- (25) Marquardt, D.; Heberle, F. A.; Miti, T.; Eicher, B.; London, E.; Katsaras, J.; Pabst, G. 1H NMR Shows Slow Phospholipid Flip-Flop in Gel and Fluid Bilayers. *Langmuir* **2017**, *33*, 3731–3741.
- (26) Nickels, J. D.; Chatterjee, S.; Stanley, C. B.; Qian, S.; Cheng, X.; Myles, D. A. A.; Standaert, R. F.; Elkins, J. G.; Katsaras, J. The in vivo structure of biological membranes and evidence for lipid domains. *PLoS Biol.* **2017**, *15*, No. e2002214.
- (27) Murugova, T. N.; Solodovnikova, I. M.; Yurkov, V. I.; Gordeliy, V. I.; Kuklin, A. I.; Ivankov, O. I.; Kovalev, Y. S.; Popov, V. I.; Teplova, V. V.; Yaguzhinsky, L. S. Potentials of Small-angle Neutron Scattering for Studies of the Structure of Live Mitochondria. *Neutron News* **2011**, *22*, 11–14.
- (28) Kučerka, N.; Nieh, M.-P.; Katsaras, J. Fluid phase lipid areas and bilayer thicknesses of commonly used phosphatidylcholines as a function of temperature. *Biochim. Biophys. Acta, Biomembr.* **2011**, *1808*, 2761–2771.
- (29) Heberle, F. A.; Marquardt, D.; Doktorova, M.; Geier, B.; Standaert, R. F.; Heftberger, P.; Kollmitzer, B.; Nickels, J. D.; Dick, R. A.; Feigenson, G. W.; Katsaras, J.; London, E.; Pabst, G. Subnanometer Structure of an Asymmetric Model Membrane: Interleaflet Coupling Influences Domain Properties. *Langmuir* **2016**, *32*, 5195–5200.
- (30) Eicher, B.; Heberle, F. A.; Marquardt, D.; Rechberger, G. N.; Katsaras, J.; Pabst, G. Joint small-angle X-ray and neutron scattering data analysis of asymmetric lipid vesicles. *J. Appl. Crystallogr.* **2017**, *50*, 419.
- (31) Nielsen, J. E.; Bjørnestad, V. A.; Lund, R. Resolving the Structural Interactions between Antimicrobial Peptides and Lipid Membranes using Small-angle Scattering Methods: the case of Indolicidin. *Soft Matter* **2018**, *14*, 8750.
- (32) Nakano, M.; Fukuda, M.; Kudo, T.; Endo, H.; Handa, T. Determination of interbilayer and transbilayer lipid transfers by time-resolved small-angle neutron scattering. *Phys. Rev. Lett.* **2007**, *98*, 238101.
- (33) Nakano, M.; Fukuda, M.; Kudo, T.; Matsuzaki, N.; Azuma, T.; Sekine, K.; Endo, H.; Handa, T. Flip-flop of phospholipids in vesicles: kinetic analysis with time-resolved small-angle neutron scattering. *J. Phys. Chem. B* **2009**, *113*, 6745–6748.
- (34) Garg, S.; Porcar, L.; Woodka, A. C.; Butler, P. D.; Perez-Salas, U. Noninvasive Neutron Scattering Measurements Reveal Slower Cholesterol Transport in Model Lipid Membranes. *Biophys. J.* **2011**, *101*, 370–377.
- (35) Sugiura, T.; Takahashi, C.; Chuma, Y.; Fukuda, M.; Yamada, M.; Yoshida, U.; Nakao, H.; Ikeda, K.; Khan, D.; Nile, A. H.; Bankaitis, V. A.; Nakano, M. Biophysical Parameters of the Sec14 Phospholipid Exchange Cycle. *Biophys. J.* **2019**, *116*, 92–103.
- (36) Wah, B.; Breidigan, J. M.; Adams, J.; Horbal, P.; Garg, S.; Porcar, L.; Perez-Salas, U. Reconciling Differences between Lipid Transfer in Free-Standing and Solid Supported Membranes: A Time-Resolved Small-Angle Neutron Scattering Study. *Langmuir* **2017**, *33*, 3384–3394.
- (37) Doktorova, M.; Heberle, F. A.; Eicher, B.; Standaert, R. F.; Katsaras, J.; London, E.; Pabst, G.; Marquardt, D. Preparation of asymmetric phospholipid vesicles for use as cell membrane models. *Nat. Protoc.* **2018**, *13*, 2086–2101.
- (38) Peyret, A.; Zhao, H.; Lecommandoux, S. Preparation and Properties of Asymmetric Synthetic Membranes Based on Lipid and Polymer Self-Assembly. *Langmuir* **2018**, *34*, 3376–3385.
- (39) Bechinger, B. Structure and functions of channel-forming peptides: Magainins, cecropins, melittin and alamethicin. *J. Membr. Biol.* **1997**, *156*, 197.
- (40) Scott, H. L.; Westerfield, J. M.; Barrera, F. N. Determination of the Membrane Translocation pK of the pH-Low Insertion Peptide. *Biophys. J.* **2017**, *113*, 869–879.
- (41) Reshetnyak, Y. K.; Segala, M.; Andreev, O. A.; Engelmann, D. M. A monomeric membrane peptide that lives in three worlds: In solution, attached to, and inserted across lipid bilayers. *Biophys. J.* **2007**, *93*, 2363–2372.
- (42) Musial-Siwek, M.; Karabazhak, A.; Andreev, O. A.; Reshetnyak, Y. K.; Engelmann, D. M. Tuning the insertion properties of pHILIP. *Biochim. Biophys. Acta, Biomembr.* **2010**, *1798*, 1041–1046.
- (43) Eicher, B.; Marquardt, D.; Heberle, F. A.; Letofsky-Papst, I.; Rechberger, G. N.; Appavou, M. S.; Katsaras, J.; Pabst, G. Intrinsic Curvature-Mediated Transbilayer Coupling in Asymmetric Lipid Vesicles. *Biophys. J.* **2018**, *114*, 146–157.
- (44) Arnold, O.; Bilheux, J. C.; Borreguero, J. M.; Buts, A.; Campbell, S. I.; Chapon, L.; Doucet, M.; Draper, N.; Ferraz Leal, R.; Gigg, M. A.; Lynch, V. E.; Markvardsen, A.; Mikkelsen, D. J.; Mikkelsen, R. L.; Miller, R.; Palmen, K.; Parker, P.; Passos, G.; Perring, T. G.; Peterson, P. F.; Ren, S.; Reuter, M. A.; Savici, A. T.; Taylor, J. W.; Taylor, R. J.; Tolchenov, R.; Zhou, W.; Zikovsky, J. Mantid - Data analysis and visualization package for neutron scattering and μ SR experiments. *Nucl. Instrum. Methods Phys. Res., Sect. A* **2014**, *764*, 156–166.
- (45) Kučerka, N.; Nieh, M.-P.; Katsaras, J. *Advances in planar lipid bilayers and liposomes*; Elsevier, 2010; Vol. 12; pp 201–235.
- (46) Qian, S.; Heller, W. T. Peptide-induced asymmetric distribution of charged lipids in a vesicle bilayer revealed by small-angle neutron scattering. *J. Phys. Chem. B* **2011**, *115*, 9831–9837.
- (47) Harroun, T. A.; Heller, W. T.; Weiss, T. M.; Yang, L.; Huang, H. W. Experimental evidence for hydrophobic matching and membrane-mediated interactions in lipid bilayers containing gramicidin. *Biophys. J.* **1999**, *76*, 937–945.
- (48) Anzai, K.; Yoshioka, Y.; Kirino, Y. Novel radioactive phospholipid probes as a tool for measurement of phospholipid translocation across biomembranes. *Biochim. Biophys. Acta, Biomembr.* **1993**, *1151*, 69–75.
- (49) Scott, H. L.; Nguyen, V. P.; Alves, D. S.; Davis, F. L.; Booth, K. R.; Bryner, J.; Barrera, F. N. The negative charge of the membrane has opposite effects on the membrane entry and exit of pH-low insertion peptide. *Biochemistry* **2015**, *54*, 1709–1712.
- (50) Nguyen, M.; DiPasquale, M.; Rickeard, B.; Stanley, C.; Kelley, E.; Marquardt, D. Methanol Accelerates DMPC Flip-Flop and Transfer: A SANS Study on Lipid Dynamics. *Biophys. J.* **2019**, *116*, 755–759.

- (51) Gilbert, R. J. C. Proteinlipid interactions and non-lamellar lipidic structures in membrane pore formation and membrane fusion. *Biochim. Biophys. Acta, Biomembr.* **2016**, *1858*, 487–499.
- (52) Rausch, J. M.; Marks, J. R.; Rathinakumar, R.; Wimley, W. C. B-Sheet pore-forming peptides selected from a rational combinatorial library: Mechanism of pore formation in lipid vesicles and activity in biological membranes. *Biochemistry* **2007**, *46*, 12124–12139.
- (53) Shai, Y. Mode of action of membrane active antimicrobial peptides. *Biopolymers* **2002**, *66*, 236–248.
- (54) Wimley, W. C. Describing the mechanism of antimicrobial peptide action with the interfacial activity model. *ACS Chem. Biol.* **2010**, *5*, 905–917.
- (55) Zoonens, M.; Reshetnyak, Y. K.; Engelman, D. M. Bilayer interactions of pHILIP, a peptide that can deliver drugs and target tumors. *Biophys. J.* **2008**, *95*, 225–235.
- (56) Huang, H. W. Molecular mechanism of antimicrobial peptides: The origin of cooperativity. *Biochim. Biophys. Acta, Biomembr.* **2006**, *1758*, 1292–1302.
- (57) Chen, F. Y.; Lee, M. T.; Huang, H. W. Evidence for membrane thinning effect as the mechanism for peptide-induced pore formation. *Biophys. J.* **2003**, *84*, 3751–3758.
- (58) De Kruijff, B.; Van Zoelen, E. J. J. Effect of the phase transition on the transbilayer movement of dimyristoyl phosphatidylcholine in unilamellar vesicles. *Biochim. Biophys. Acta, Biomembr.* **1978**, *511*, 105–115.
- (59) Reshetnyak, Y. K.; Andreev, O. A.; Segala, M.; Markin, V. S.; Engelman, D. M. Energetics of peptide (pHLIP) binding to and folding across a lipid bilayer membrane. *Proc. Natl. Acad. Sci. U. S. A.* **2008**, *105*, 15340–15345.